Solid Freeform Fabrication 2022: Proceedings of the 33rd Annual International Solid Freeform Fabrication Symposium – An Additive Manufacturing Conference
Reviewed Paper

Investigation of Wear Behavior of Centrifugal Disc Finishing on Additively Manufactured Ti6Al4V Samples

Foxian Fan[1], Sagar Jalui[2], Nicholas Lajoie[3], Guha Manogharan[2,3*]

[1]*Department Industrial & Manufacturing Engineering, The Pennsylvania State University, University Park, PA, U.S.A.*

[2]*Department of Mechanical Engineering, University Park, The Pennsylvania State University, University Park, PA, U.S.A.*

[3]*Additive Manufacturing and Design, World Campus, The Pennsylvania State University*

*Corresponding author: gum53@psu.edu

Abstract

As-built Additively Manufactured (AM) metallic parts require secondary processing in most applications to improve surface finish and mechanical strength. Mass Finishing (MF) processes are gaining popularity as effective and economical surface improvement methods for metal AM parts. This study investigates the wear behavior of post-processing both Laser Powder Bed Fusion (LPBF) and Electron Beam Melting (EBM) fabricated Ti6Al4V parts via Centrifugal Disc Finishing (CDF). Both AM orientation-based surface finish and wear behavior are compared for better understanding on key mechanisms of AM+MF hybrid manufacturing system. The areal surface roughness results showed that wear rate on side surfaces were higher than top surfaces for both LPBF and EBM samples in CDF. In addition, LPBF samples exhibited higher material removal than EBM samples based on weight loss measurements.

Keyword: AM Post-Processing, AM Areal Surface Roughness, Mass Finishing, Centrifugal Disc Finishing, AM Wear Behavior, Hybrid Manufacturing

Introduction

Despite the rapid development of Additive Manufacturing (AM) in recent years, poor surface roughness of as built metal-AM parts remains as one of the most critical challenges. [1]-[4]. It is common knowledge that surface roughness greatly affects not only aesthetic view, but also fatigue life, corrosion resistance, and functionality. As a result, AM post processing, especially surface treatment, becomes one of the major cost factors in the entire production process. Popular surface finishing methods such as CNC machining can drastically improve the surface roughness but restrict the design freedom of AM.

Mass Finishing (MF) technologies are capable of batch processing workpieces. Furthermore, fixtureless MF methods, such as Centrifugal Disc Finishing (CDF), offer more design freedom in both geometry and size for AM. As a result, using MF methods to improve AM surface roughness is gaining popularity in recent years. Jamal et al., [5] investigated the effectiveness of using four types of MF machines to improve surface finish of LPBF Ti6Al4V

parts. Despite the differences between achieved resultant roughness, all four types of MF machines effectively improved the surface finishes. Typical MF processes are abrasive media-based deburring processes that might require a fixture to hold workpieces. The abrasive media perform micro-cutting on the workpiece and removes the "peaks" on the surfaces. [6]-[9] In recent development of AM + MF, Boschetto et al., [10] investigated the surface roughness and radii effects of SLM Ti6Al4V parts in barrel finishing. Kaynak et al., [11] investigated the difference of wear behavior when processing LPBF Inconel 718 in finish machining and disc finishing, which about seven and twelve percent wear rate reduction was observed in comparison to as-built samples. While many material removal/wear rate prediction models were developed for several types of Mass Finishing methods, [6], [7], [12]–[16], Malkorra et al., [17] developed a numerical model for AM + Drag Finishing for SLM Ti4Al6V. However, few studies have investigated the AM surface orientation specified wear behavior despite the significant differences in initial surface roughness between them. Reciprocating wear tests were conducted between 90° build over-hang "side surface" and flat "top surface" on Electron Beam Melting (EBM) Ti6Al4V samples in a study conducted by Shrestha [18]. This study found that wear behavior of AM surface are build-orientation dependent, where "top surface" exhibits less wear volume in comparison to "side surface". Since MF improves surface finish by micro cutting surface burrs, it is unclear if these observations hold true in AM + MF scenario. In addition, Li et al., [19] found no significant difference between wear rate in LPBF and EBM samples during a reciprocating wear test, which the wear rates were unaffected in high hardness LPBF samples and lower hardness EBM samples. In the previous study [8], the relationship between resultant surface roughness, rotational speed, and processing time of CDF processed LPBFTi6Al4V parts was statistically investigated. As a continuation, this study aims to investigate the following questions to fill in the existing research questions of AM + MF system:

- Does the AM Ti6Al4V build orientation (top v/s side surface) affect wear behavior in Centrifugal Disc Finishing?
- Does AM Ti6Al4V fabricated using LPBF and EBM Ti6Al4V have different material removal rate in Centrifugal Disc Finishing?

It should be noted that material removal rate is frequently interchangeable with wear rate in many applications. In this study, the wear rate in this study refer to the particular surface wear rate base on surface roughness change over time, while material removal rate refers to the global weight loss over time for a particular sample.

Design and Experiment

Three Ti-64 LPBF samples with dimensions 0.5” x 0.5” x 1” (12.7 mm x 12.7 mm x 25.4 mm) were fabricated using the 3D Systems ProX 320 system with layer thickness of 60 µm, laser power of 245 W and hatch spacing of 82 µm. Six Ti-64 EBM samples with dimensions 0.5” x 0.5” x 1” (12.7 mm x 12.7 mm x 25.4 mm) were fabricated using the Arcam Q20+ system with layer thickness of 90 µm, beam current of 2 mA at speed function setting 6. (Figure 1) The Ti-64 powder used is Grade 23 with nominal size of 15-45 µm for LPBF, and nominal size of 45-105 µm powder for EBM. Three out of these six samples were produced using multi-spot capabilities withing the Q20+ using 70 spots. Lattice support structures were added to the EBM samples. In order to remove the lattice support structures on the EBM parts and ensure geometrically similar parts all the support structures were sawed off, and face milling was performed on 3 surfaces. The preparation process left two side surfaces and the top surface in as-built condition. Additionally, the YZ surfaces (Figure 1.) on three samples were further polished with (grit 2000) sandpaper after face-milling for Vickers Hardness Test.

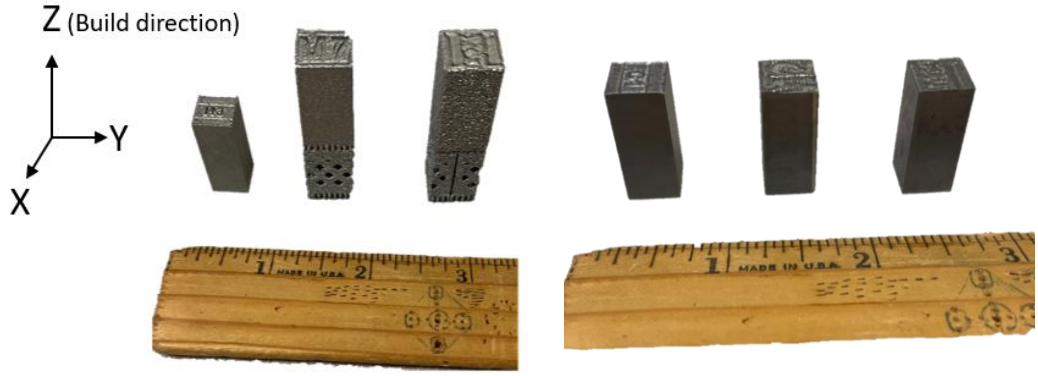

Figure 1: *As-built LPBF, multi-spot EBM, and standard EBM (left); machined LPBF, multi-spot EBM, and standard EBM (right)*

CDF operations were performed using the Walther Trowal TT-45 Centrifugal Disc Finisher, with 3 mm diameter spherical ceramic abrasive media purchased from Algrium. (Figure 2) The same batch of media were used repeatedly through the whole experiment. The lubricant used was a mixture of commercially available formula, Trowal KFL, and water (~1:100000). CDF operations were performed on each fabricated samples for a full factorial design of experiments: 30, 60, 90, and 180 mins at 150, 200, and 250 RPM.

***Figure 2**: Walther Trowal TT-45 Centrifugal Disc Finisher with the 3 mm diameter spherical media*

As-built and processed surface roughness measurements were taken using the Zygo NexView 3D optical profilometer with a primary magnification of 20X and internal magnification of 1X, resulting in a measurement patch of roughly 400 µm X 400 µm. Two indents (diagonal ends) were marked on the XY and XZ surfaces of every sample to ensure the measurement region remains consistent. A resultant 1 mm X 1mm stitched patch pattern was selected consisting of a grid of 3 x 3 patches of 400 µm X 400 µm with 20% overlap using the Zygo MX software. Form removal was used with an order of 4, followed by Robust Gaussian Spline filter with cut-off wavelength of 2.5 mm to obtain the filtered roughness profile. Data filling was used for visualization only. The parameters of interest which were exported included arithmetic areal surface roughness (S_a), peak-to-valley height (S_z), reduced peak height (S_{pk}), and reduced peak volume (V_{mp}). Vickers Hardness values were collected on polished as-built samples as shown in Table 1 and Figure 3.

The surface roughness data were collected after 30-, 60-, 90-, and 180-minutes processing time on both top and side surfaces of each sample. Weight of the as-built and processed samples were recorded after each run as well with a weighing scale with a 0.002 g deviation.

***Table 1:** Vickers hardness values measured for as-built parts*

Sample	Hardness Mean	Number of Measurements	Standard Dev.
L-PBF	432 HV1	10	5.2
M-EBM	376 HV1	10	8.66
NM-EBM	370 HV1	10	18.09

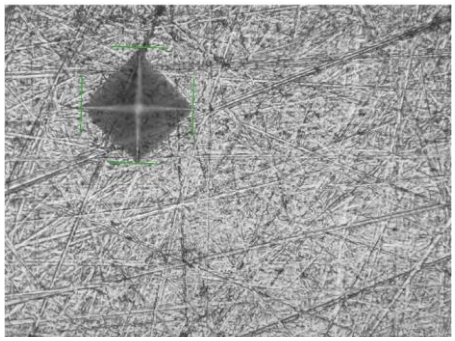

***Figure 3:** Vickers microhardness were collected on the polished side surfaces of all AM samples using diamond indentation*

The LPBF samples are labeled as Laser 1-3; the multi-spot EBM samples are labeled as M-EBM 1-3; and the standard EBM samples are labels as EBM 1-3. Only processing time and disc spinning speed are changed through the experiment as shown in Table 2.

***Table 2**: Design of experiments for Centrifugal Disc Finishing*

Sample	Processing Time(min)	Speed (RPM)
Laser 1, M-EBM1, EBM 1	0, 30, 60, 90, 180	150
Laser 2, M-EBM 2, EBM2	0, 30, 60, 90, 180	200
Laser 3, M-EBM 3, EBM3	0, 30, 60, 90, 180	250

Data Analysis and Discussion

In AM, contour build side surface and melt pool formed top surface result in different surface roughness, where the side surface is prone to higher roughness than the top surface. In many surface improvement processes, higher initial roughness result in more surface roughness reduction. Therefore, to investigate if the wear behavior between high roughness side surface and low roughness top surface are different in CDF, the S_a, S_z, S_{pk}, and V_{mp} are compared, where S_{pk} and V_{mp} are typically used for wear analysis as mentioned in [20]. The boxplot of all collected S_{pk} and V_{mp} data, separated based on top and side surface, of each sample are summarized in Figure 4-7. One way ANOVA with Tukey Pairwise Comparison was performed within all samples. Remaining S_a and S_z data plots are presented in the Appendix.

Reductions in S_a, S_z, S_{pk}, and V_{mp} were observed across all samples on both surfaces over different processing time periods. One-way ANOVA was performed between time period groups and control groups for S_a, S_z, S_{pk}, and V_{mp}. It was observed that the overall reduction in S_a, S_z, S_{pk}, and V_{mp} were consistently significant for side surfaces across all samples. It was also noted that significant reduction of S_a, S_z, S_{pk}, and V_{mp} were observed for both top and side surface for standard build EBM samples. The overall occurrences of significant surface roughness reduction of side surfaces were higher than top surfaces for all AM samples. This phenomenon was also visualized in white light profilometer reconstructed 3D surface in Figure 12 -14, where side surfaces experienced more visual detectable wear than top surfaces over time for all AM samples.

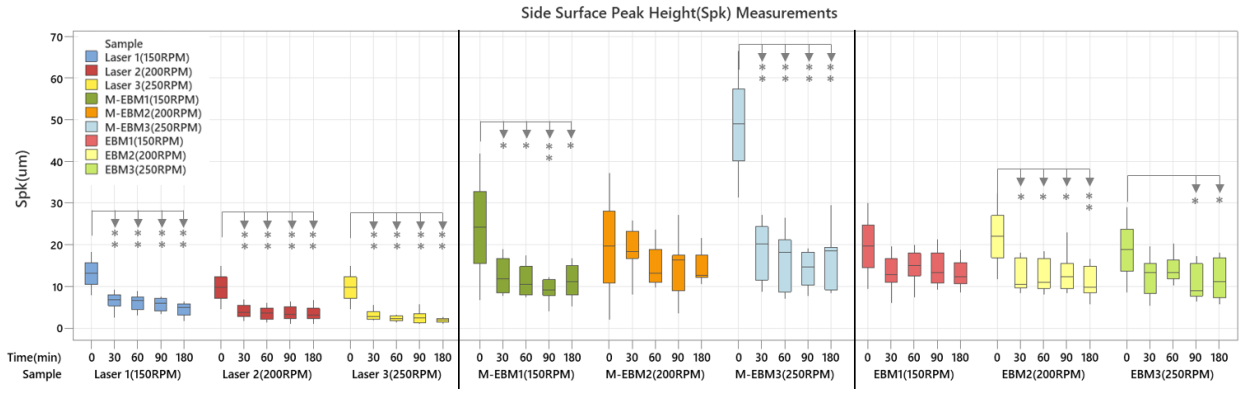

Figure 4. *Side surface S_{pk} measurement from as build condition to 30, 60, 90, and 180 minutes processing time under 150, 200, &250 RPM disc rotation speed. Arrow pointer refers to one-way ANOVA of Tukey Pairwise Comparisons: * indicates P<0.05; ** indicates P < 0.01. All other comparisons with P > 0.05 are not indicated.*

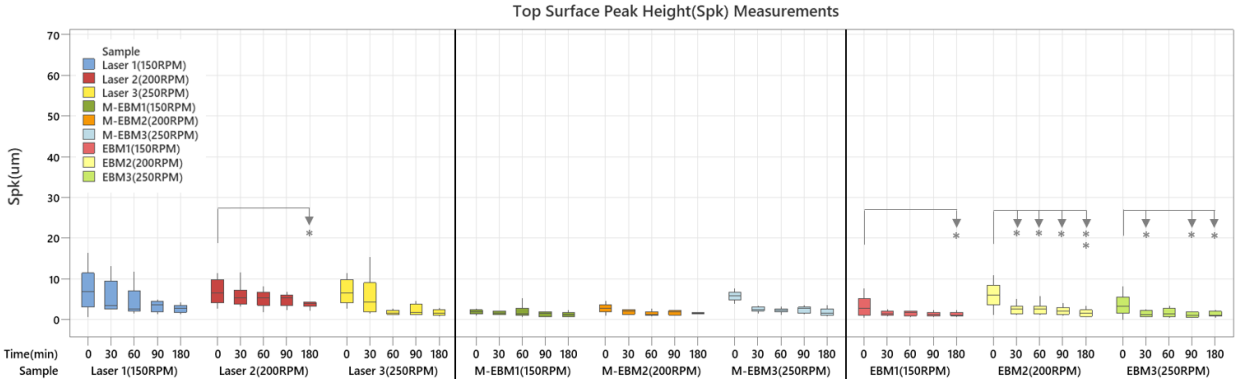

Figure 5. *Top surface S_{pk} measurement from as build condition to 30, 60, 90, and 180 minutes processing time under 150, 200, &250 RPM disc rotation speed. Arrow pointer refers to one-way ANOVA of Tukey Pairwise Comparisons: * indicates P<0.05; ** indicates P < 0.01. All other comparisons with P > 0.05 are not indicated.*

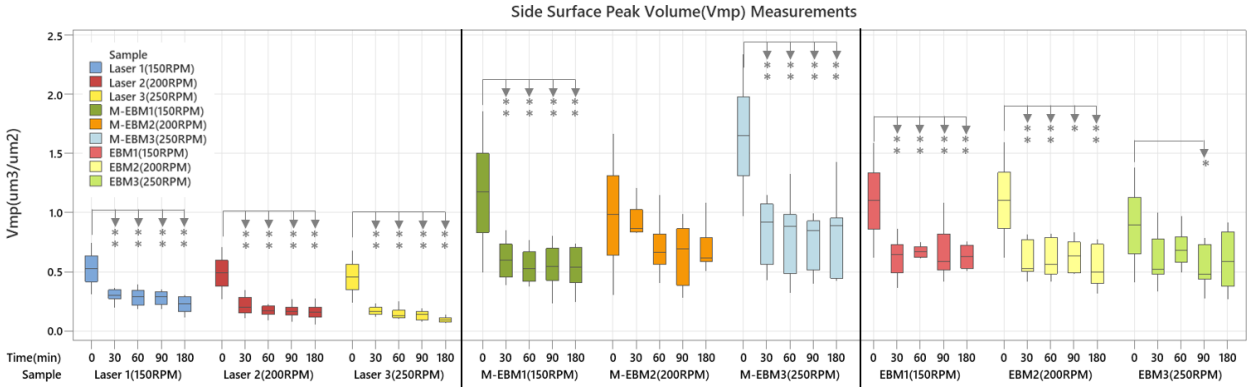

Figure 6. *Side surface V_{mp} measurement from as build condition to 30, 60, 90, and 180 minutes processing time under 150, 200, &250 RPM disc rotation speed. Arrow pointer refers to one-way ANOVA of Tukey Pairwise Comparisons: * indicates P<0.05; ** indicates P < 0.01. All other comparisons with P > 0.05 are not indicated.*

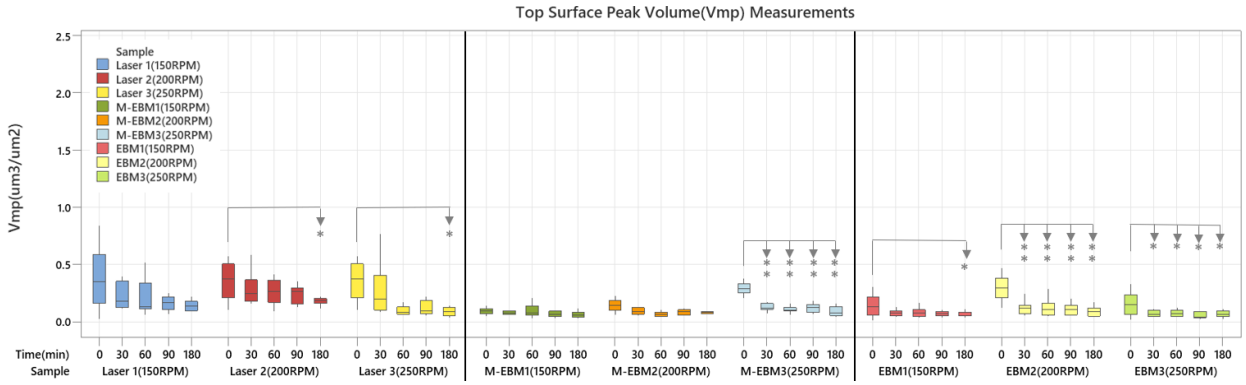

Figure 7. *Top surface V_{mp} measurement from as build condition to 30, 60, 90, and 180 minutes processing time under 150, 200, &250 RPM disc rotation speed. Arrow pointer refers to one-way ANOVA of Tukey Pairwise Comparisons: * indicates P<0.05; ** indicates P < 0.01. All other comparisons with P > 0.05 are not indicated.*

Vickers Hardness tests were conducted on face-milled then fine polished as-built samples. (Figure. 3) Percentage weight loss was used to determine if the initial hardness of different AM fabrication methods affects wear behavior in CDF. Based on collected weight loss data as shown in Figure. 15, it is evident that higher hardness LPBF samples have higher wear rate in comparison to lower hardness EBM samples. Li et al., [19] found no differences in wear rate between LPBF and EBM samples in the reciprocating wear test. However, the difference observed in this study can be attributed to the differences in AM setting: (1) The EBM samples were fabricated on pre-sintered powder as compared to LPBF samples. Thus, excessive amounts of partially melted loose powder were attached to the surfaces of LPBF samples. As a result, most material removal was attributed to removal of such partially melted loose powder. (2) The LPBF parts had smaller printing resolution than EBM, which resulted in vastly different surface features. Also, on the side surfaces, the ridges on EBM samples were larger than LPBF samples. These phenomena were also captured via reconstructed 3D pictures from the white light profilometer. (Figure. 8-10) Furthermore, due to the fact that surface features drastically affect the hardness measurement process, the Vickers Hardness measurements were collected on milled and finely polished surfaces, which do not directly reflect the true strength of the as-built stratified surface. Due to the above reasons, LPBF samples exhibited slightly higher material removal rate than EBM samples during the period of processing time.

As expected, increasing processing speed also resulted in higher material removal rate, due to more aggressive abrasion between media and workpieces. Most material removal happened within the first 30 minutes; the material removal rate starts to decrease after 30 minutes. This result was consistent with the general knowledge of MF where the transient period has aggressive material removal while steady state period has gradual material removal.[16] Additional One-way ANOVA with Tukey Pair-wise Comparison was performed to identify how disc spinning speed affects the top surface and side surface under same processing time. Similarly, the boxplot of S_{pk} and V_{mp} data, separated based on top and side surface, of each sample are summarized (Figure.8-11) Remaining S_a and S_z data plots are presented in the Appendix. It was found that: (1). Despite

the differences of initial surface roughness on each sample, increasing disc spinning speed only proportionally affected the wear rate of side surfaces on L-PBF samples; (2). Top surfaces were unaffected by disc speed changes for all AM samples; (3). Both top and side surfaces of EBM and M-EBM samples were unaffected by disc speed changes. This result also helped to explain why L-PBF samples exhibited higher material removal than all EBM and M-EBM samples as shown in Figure. 15. Most wear was observed on the side surfaces of L-PBF samples, due to the large amounts of partially melted powder. Increasing disc rotation speed resulted in increasing wear rate on L-PBF side surfaces and thus, material removal on side surfaces.

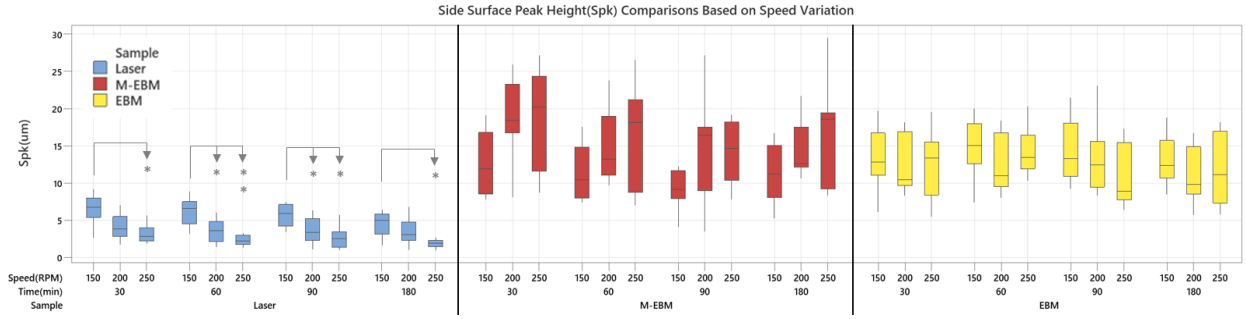

Figure 8. *Side surface S_{pk} measurement between 150, 200, &250 RPM disc rotation speed under same processing time. Arrow pointer refers to one-way ANOVA of Tukey Pairwise Comparisons: * indicates P<0.05; ** indicates P < 0.01. All other comparisons with P > 0.05 are not indicated.*

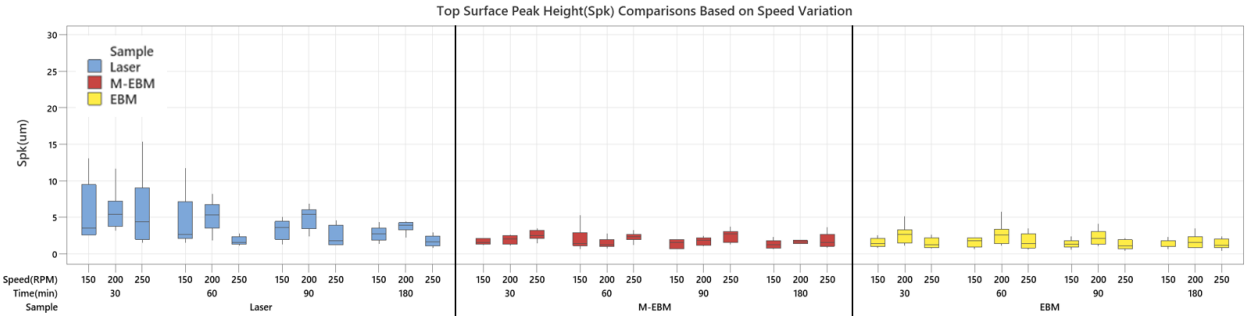

Figure 9. *Top surface S_{pk} measurement between 150, 200, &250 RPM disc rotation speed under same processing time. Arrow pointer refers to one-way ANOVA of Tukey Pairwise Comparisons: * indicates P<0.05; ** indicates P < 0.01. All other comparisons with P > 0.05 are not indicated.*

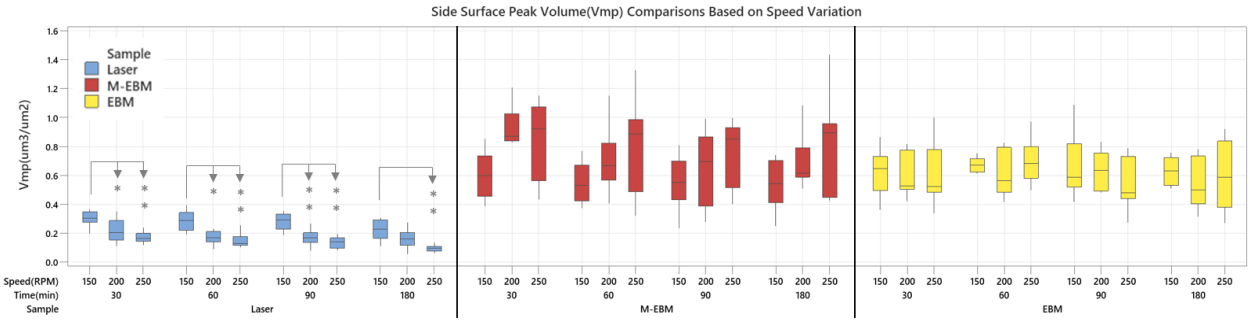

Figure 10. *Side surface V_{mp} measurement between 150, 200, &250 RPM disc rotation speed under same processing time. Arrow pointer refers to one-way ANOVA of Tukey Pairwise Comparisons: * indicates P<0.05; ** indicates P < 0.01. All other comparisons with P > 0.05 are not indicated.*

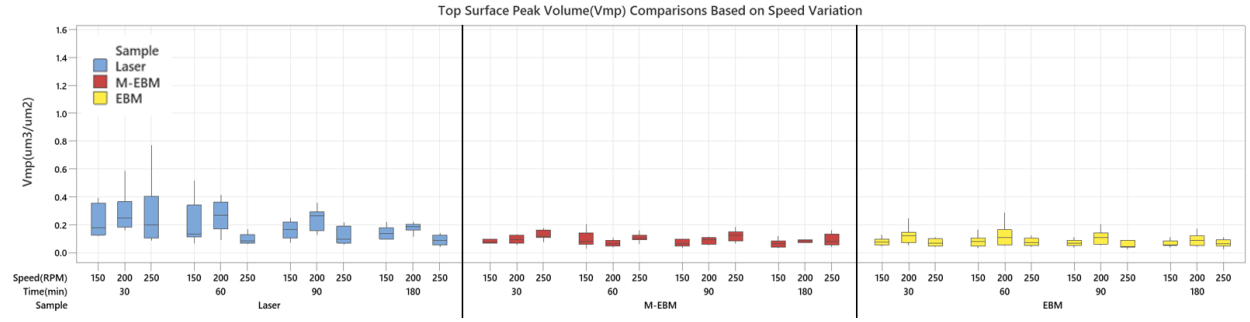

Figure 11. *Top surface V_{mp} measurement between 150, 200, &250 RPM disc rotation speed under same processing time. Arrow pointer refers to one-way ANOVA of Tukey Pairwise Comparisons: * indicates P<0.05; ** indicates P < 0.01. All other comparisons with P > 0.05 are not indicated.*

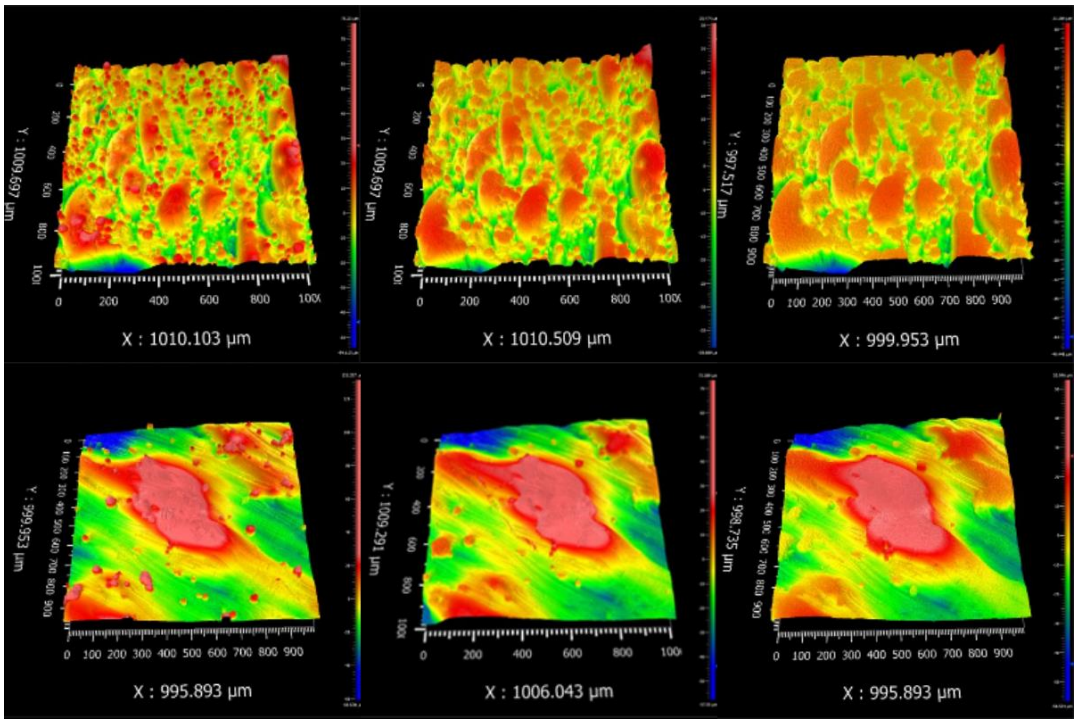

Figure 12. *White light profilometer constructed 3D surface of Laser Powder Bed Fusion samples. Top three from left to right: as-built side surface, 30 min processed side surface, and 180 min processed side surface. Bottom three from left to right: as-built top surface, 30 min processed top surface, and 180 min processed surface.*

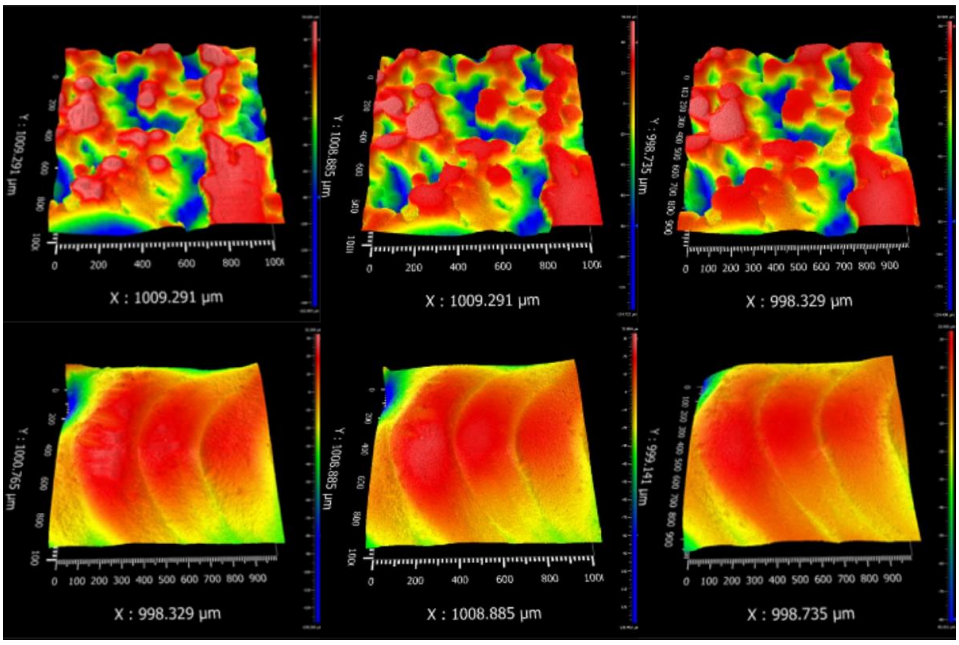

Figure 13. *White light profilometer constructed 3D surface of Multi-spot EBM samples. Top three from left to right: as-built side surface, 30 min processed side surface, and 180 min processed side surface. Bottom three from left to right: as-built top surface, 30 min processed top surface, and 180 min processed surface.*

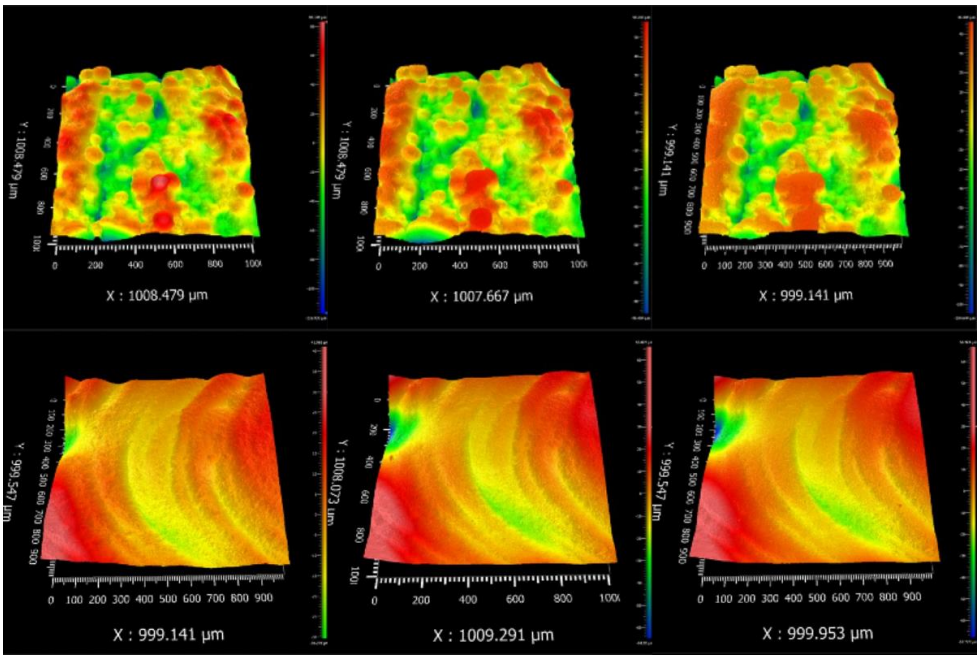

Figure 14. *White light profilometer constructed 3D surface of standard EBM samples. Top three from left to right: as-built side surface, 30 min processed side surface, and 180 min processed side surface. Bottom three from left to right: as-built top surface, 30 min processed top surface, and 180 min processed surface.*

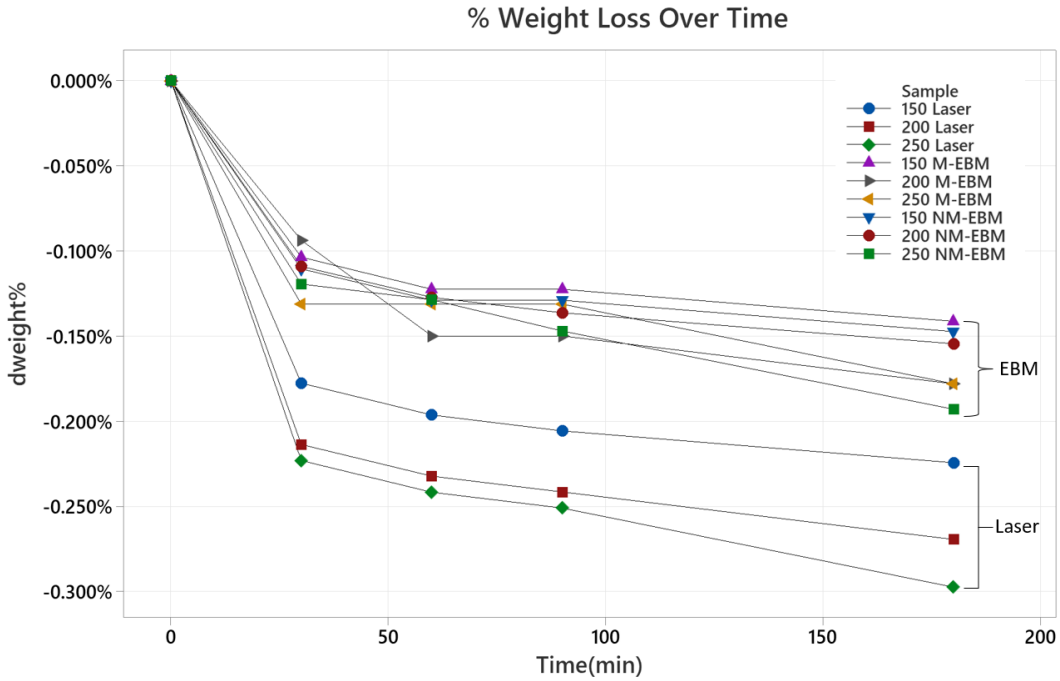

Figure 15. *Percentage weight loss of all AM samples over time.*

Conclusion

This original study involved fabricating LPBF, M-EBM and standard EBM Ti6Al4V samples, which were subjected to different processing parameters of CDF. AM orientation-based wear rate of surfaces were compared using areal surface roughness parameters. It was found that the side surfaces (higher initial roughness) of all AM samples showed statistically significant reduction of S_a, S_z, S_{pk}, and V_{mp} in most cases as compared to top surfaces (lower initial roughness). In addition, effects of disc rotation speed on top vs. side surface wear behavior were also studied. It was found that only the side surfaces of L-PBF samples are directly proportional to increasing disc rotation speed. Top surfaces of all AM samples, and all surfaces of EBM and M-EBM samples were unaffected by changing rotation speed. This result also indicated that most material removal of L-PBF samples are contributed by wearing-off side surfaces' partially melted powder.

Material removal rate were also compared between LPBF (higher initial hardness), and EBM (lower initial hardness) samples based on percentage weight loss over time, where LPBF showed higher material removal rate than EBM samples. This result can be due to the following reasons:

- As-built LPBF surface contains substantial amounts of partially melted powder, which were easier to remove during the CDF process. Additionally, different printing resolutions between LPBF and EBM result in drastically different surface features, where LPBF samples have smaller and thinner ridges on side surfaces than EBM samples.
- The Vickers Hardness values were collected on machined AM surfaces, which does not reflect the true strength of the as-built AM surfaces.

Future work includes developing material removal based resultant surface roughness prediction model for CDF processed metal AM parts and evaluate economic efficiency of AM + MF hybrid manufacturing system through a cost prediction model.

Acknowledgement

The authors acknowledge Penn State FAME lab staff Travis Richner and Brent Johnston for their support.

References

[1] Chong, L., Ramakrishna, S., & Singh, S. (2018). A review of digital manufacturing-based hybrid additive manufacturing processes. *The International Journal of Advanced Manufacturing Technology*, *95*(5), 2281-2300.

[2] Gong, X., Zeng, D., Groeneveld-Meijer, W., & Manogharan, G. P. (2022). Additive manufacturing: A machine learning model of process-structure-property linkages for machining behavior of Ti-6Al-4V. *Mater Sci Add Manuf*, *1*(6).

[3] Dilberoglu, U. M., Gharehpapagh, B., Yaman, U., & Dolen, M. (2021). Current trends and research opportunities in hybrid additive manufacturing. *The International Journal of Advanced Manufacturing Technology*, *113*(3), 623-648.

[4] Iquebal, A. S., Shrestha, S., Wang, Z., Manogharan, G. P., Bukkapatnam, S., & Youngstown, O. (2016). Influence of milling and non-traditional machining on surface properties of Ti6Al4V EBM components. In *Proceedings of the 2016 Industrial and Systems Engineering Research Conference*.

[5] Jamal, M., & Morgan, M. N. (2017). Design process control for improved surface finish of metal additive manufactured parts of complex build geometry. *Inventions*, *2*(4), 36.

[6] Domblesky, J., Evans, R., & Cariapa, V. (2004). Material removal model for vibratory finishing. *International journal of production research*, *42*(5), 1029-1041.

[7] Uhlmann, E., Dethlefs, A., & Eulitz, A. (2014). Investigation of material removal and surface topography formation in vibratory finishing. *Procedia CIRP*, *14*, 25-30.

[8] Fan, F., Soares, N., Jalui, S., Isaacson, A., Savla, A., Manogharan, G., & Simpson, T. (2021). Effects of Centrifugal Disc Finishing for Surface Improvements in Additively Manufactured Gears. In *2021 International Solid Freeform Fabrication Symposium*. University of Texas at Austin.

[9] Gillespie, L. (2006). *Mass finishing handbook*. Industrial Press.

[10] Boschetto, A., Bottini, L., & Veniali, F. (2018). Surface roughness and radiusing of Ti6Al4V selective laser melting-manufactured parts conditioned by barrel finishing. *The International Journal of Advanced Manufacturing Technology*, *94*(5), 2773-2790.

[11] Kaynak, Y., & Tascioglu, E. (2020). Post-processing effects on the surface characteristics of Inconel 718 alloy fabricated by selective laser melting additive manufacturing. *Progress in Additive Manufacturing*, *5*(2), 221-234.

[12] Cariapa, V., Park, H., Kim, J., Cheng, C., & Evaristo, A. (2008). Development of a metal removal model using spherical ceramic media in a centrifugal disk mass finishing machine. *The International Journal of Advanced Manufacturing Technology*, *39*(1), 92-106.

[13] Makiuchi, Y., Hashimoto, F., & Beaucamp, A. (2019). Model of material removal in vibratory finishing, based on Preston's law and discrete element method. *CIRP Annals*, *68*(1), 365-368.

[14] Uhlmann, E., Eulitz, A., & Dethlefs, A. (2015). Discrete element modelling of drag finishing. *Procedia CIRP*, *31*, 369-374.

[15] Mullany, B., Shahinian, H., Navare, J., Azimi, F., Fleischhauer, E., Tkacik, P., & Keanini, R. (2017). The application of computational fluid dynamics to vibratory finishing processes. *CIRP Annals*, *66*(1), 309-312.

[16] Uhlmann, E., Dethlefs, A., & Eulitz, A. (2014). Investigation into a geometry-based model for surface roughness prediction in vibratory finishing processes. *The International Journal of Advanced Manufacturing Technology*, *75*(5), 815-823.

[17] Malkorra, I., Souli, H., Salvatore, F., Arrazola, P., Rech, J., Mathis, A., & Rolet, J. (2022). Numerical modelling of the drag finishing process at a macroscopic scale to optimize surface roughness improvement on additively manufactured (SLM) Inconel 718 parts. *Procedia CIRP*, *108*, 648-653.

[18] Shrestha, S. (2017). *Wear behavior of Ti-6Al-4V for joint implants manufactured by electron beam melting*. Youngstown State University.

[19] Li, H., Ramezani, M., & Chen, Z. W. (2019). Dry sliding wear performance and behaviour of powder bed fusion processed Ti–6Al–4V alloy. *Wear*, *440*, 203103.

[20] Leach, R. (Ed.). (2013). *Characterisation of areal surface texture*. Springer Science & Business Media.

Appendix

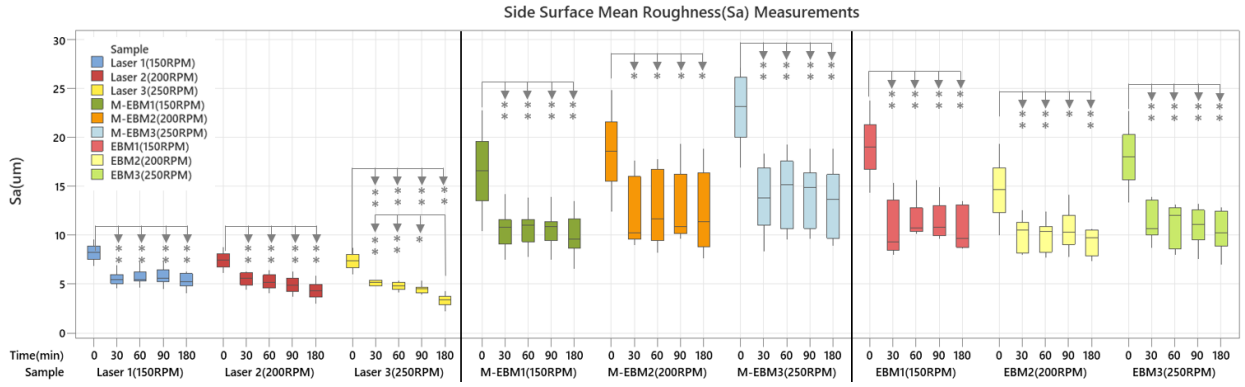

Figure 16*. Side surface Sa measurement from as build condition to 30, 60, 90, and 180 minutes processing time under 150, 200, &250 RPM disc rotation speed. Arrow pointer refers to one-way ANOVA of Tukey Pairwise Comparisons: * indicates P<0.05; ** indicates P < 0.01. All other comparisons with P > 0.05 are not indicated.*

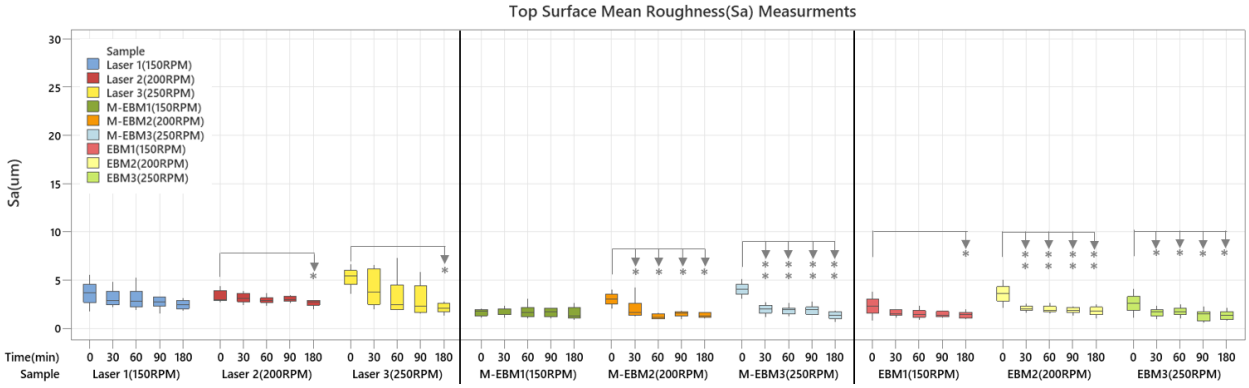

Figure 17*. Top surface Sa measurement from as build condition to 30, 60, 90, and 180 minutes processing time under 150, 200, &250 RPM disc rotation speed. Arrow pointer refers to one-way ANOVA of Tukey Pairwise Comparisons: * indicates P<0.05; ** indicates P < 0.01. All other comparisons with P > 0.05 are not indicated.*

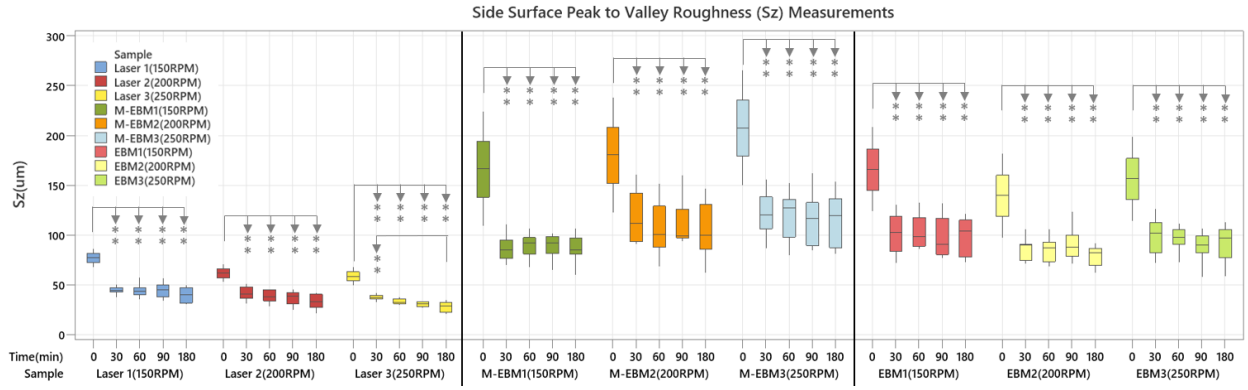

Figure 18. *Side surface Sz measurement from as build condition to 30, 60, 90, and 180 minutes processing time under 150, 200, &250 RPM disc rotation speed. Arrow pointer refers to one-way ANOVA of Tukey Pairwise Comparisons: * indicates P<0.05, ** indicates P < 0.01. All other comparisons with P > 0.05 are not indicated.*

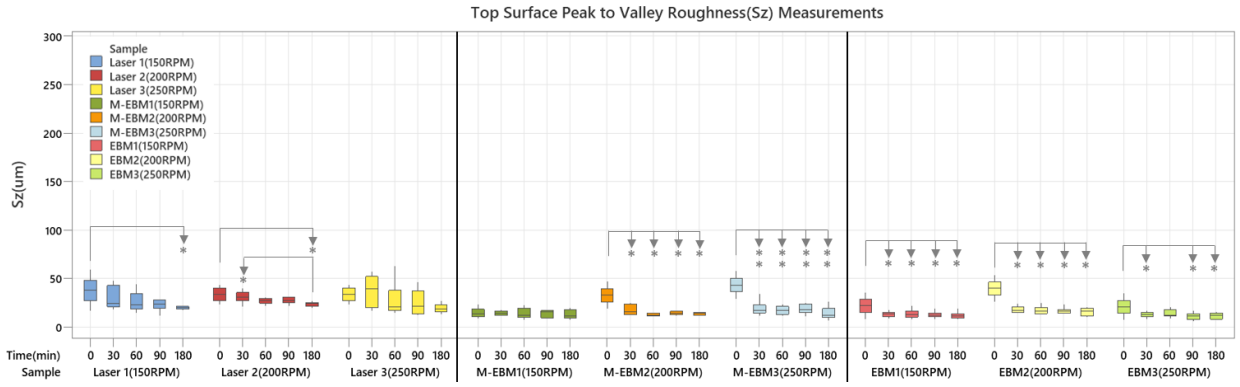

Figure 19. *Top surface Sz measurement from as build condition to 30, 60, 90, and 180 minutes processing time under 150, 200, &250 RPM disc rotation speed. Arrow pointer refers to one-way ANOVA of Tukey Pairwise Comparisons: * indicates P<0.05, ** indicates P < 0.01. All other comparisons with P > 0.05 are not indicated.*

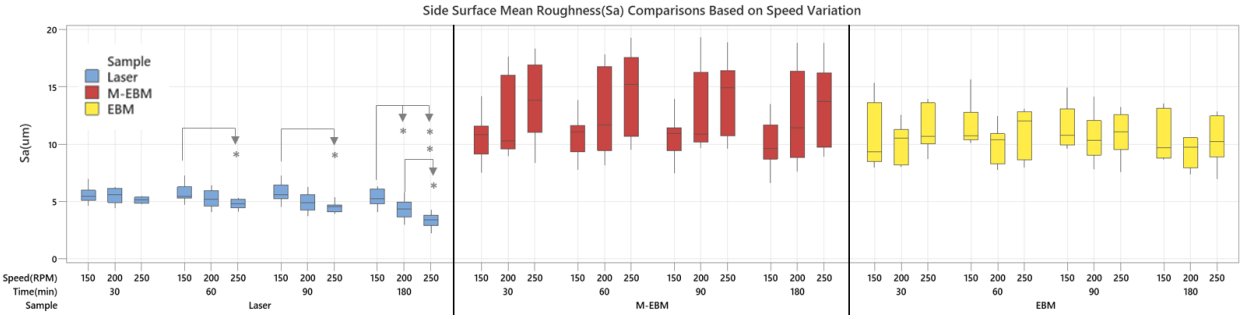

Figure 20*. Side surface Sa measurement between 150, 200, &250 RPM disc rotation speed under same processing time. Arrow pointer refers to one-way ANOVA of Tukey Pairwise Comparisons: * indicates P<0.05; ** indicates P < 0.01. All other comparisons with P > 0.05 are not indicated.*

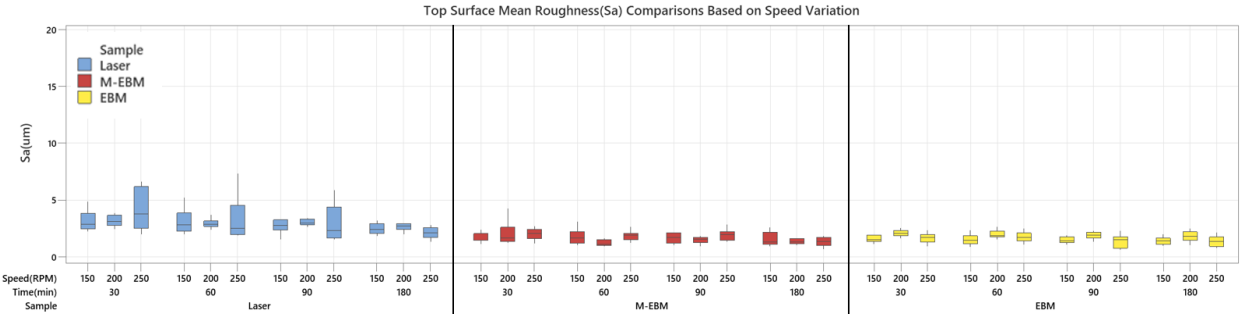

Figure 21. *Top surface Sa measurement between 150, 200, &250 RPM disc rotation speed under same processing time. Arrow pointer refers to one-way ANOVA of Tukey Pairwise Comparisons: * indicates P<0.05; ** indicates P < 0.01. All other comparisons with P > 0.05 are not indicated.*

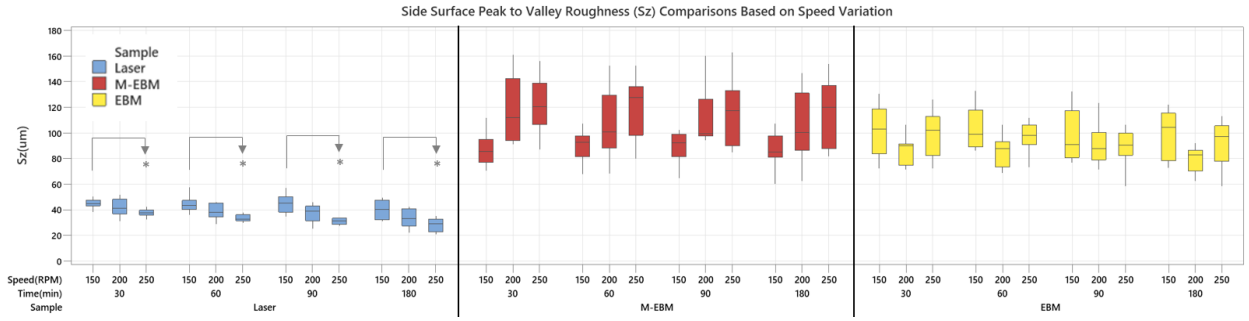

Figure 22. *Side surface Sz measurement between 150, 200, &250 RPM disc rotation speed under same processing time. Arrow pointer refers to one-way ANOVA of Tukey Pairwise Comparisons: * indicates P<0.05; ** indicates P < 0.01. All other comparisons with P > 0.05 are not indicated.*

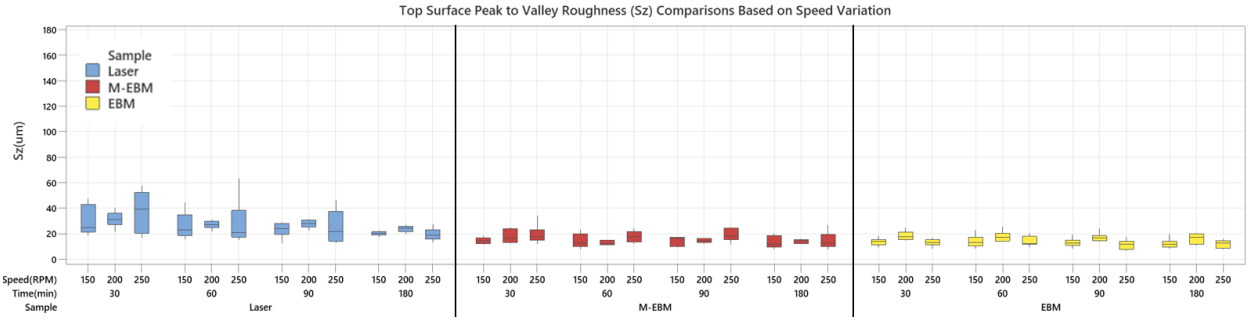

Figure 23. *Top surface Sz measurement between 150, 200, &250 RPM disc rotation speed under same processing time. Arrow pointer refers to one-way ANOVA of Tukey Pairwise Comparisons: * indicates P<0.05; ** indicates P < 0.01. All other comparisons with P > 0.05 are not indicated.*